American Mineralogist, Volume 90, pages 101–114, 2005

Allanite and epidote weathering at the Coweeta Hydrologic Laboratory, western North Carolina, U.S.A.

JASON R. PRICE,* MICHAEL A. VELBEL, AND LINA C. PATINO

Department of Geological Sciences, 206 Natural Science Building, Michigan State University, East Lansing, Michigan 48824-1115, U.S.A.

ABSTRACT

Allanite and epidote occur in the parent rocks of weathered regolith at the Coweeta Hydrologic Laboratory in North Carolina and exhibit different responses to weathering. Petrographically, epidote and allanite are identical at Coweeta, and only with additional analytical techniques (e.g., EDS or LA-ICP-MS) can the two be distinguished. Allanite is more abundant in unweathered bedrock but weathers readily below the weathering front. In contrast, the much less abundant epidote persists into the solum with only minimal evidence of weathering. The rapid dissolution of allanite is likely influenced by its metamict nature. Both epidote and allanite at Coweeta dissolve by interface-controlled dissolution kinetics, evidenced by etch pits on grain surfaces. Etch pits appear to be either large "negative crystals," or small, shallow, and elongated. The incipient stage of allanite weathering is characterized by Al mobility and Fe precipitation as goethite. During the initial stage of allanite weathering, carbonate precipitates, but with progressive weathering the carbonate is dissolved.

Based on electron microprobe analyses and point-count data of the Ca-bearing phases in the Coweeta bedrock, accessory (<1%) allanite contains a minimum of approximately 25% of the total bedrock Ca by volume, whereas garnet and plagioclase contain 5% and 70%, respectively. Although allanite and epidote are Ca-hosts, only allanite is present in significant quantities, and is weathering sufficiently rapidly, to serve as an important source of Ca in pore and stream waters at Coweeta. Allanite weathering should, therefore, be evaluated in weathering studies of crystalline silicate bedrock, especially where other lines of evidence indicate the need to invoke additional Ca sources.

INTRODUCTION

Epidote and allanite are isostructural and belong to the epidote-group of sorosilicate minerals. The ideal formula is $A_2M_3Si_3O_{12}OH$, where the A sites contain large, high-coordination-number cations such as Ca, Sr, lanthanides, etc., and the M sites are occupied by octahedrally coordinated, trivalent and occasionally divalent cations such as Al, Fe^{3+}, Mn^{3+}, Fe^{2+}, Mg, etc. (Dollase 1971). Epidote and allanite are common as accessory phases in crystalline silicate rocks and are significant hosts of Ca. If dissolved during weathering, epidote and allanite may release abundant Ca to pore waters, in addition to Al and Si.

The behavior of epidote during weathering has been a topic of controversy. Epidote is a common constituent of the heavy mineral fraction of clastic sediments (e.g., Frye et al. 1960; Willman et al. 1963; Carver 1986; Friis 1974; Poppe et al. 1995; Dill 1995; Logan and Dyer 1996; Uddin and Lundberg 1998; Khan and Kim 1998; Cocker 1998) and the residual mineral fraction of soils (e.g., Suwa et al. 1958; Gupta and Talwar 1997; Ezzaïm et al. 1999). The persistence of epidote in naturally weathered materials has been compared to that of quartz (Allen and Hajek 1995, their Table 4-1) and zircon (Lång 2000). In contrast, rapid dissolution of epidote has been invoked in modeling studies of mineral weathering and solute production (Sverdrup 1990; Oliva et al. 2004), and epidote has been included with plagioclase, K-feldspar, hornblende, and apatite, as being the major mineralogic controls for calculation of field weathering rates using the PROFILE model (Warfvinge and Sverdrup 1992; Sverdrup and Warfvinge 1993, 1995; and references contained therein). These authors routinely include epidote in model-derived field weathering rate calculations, but do so without any mineralogic observations to support its occurrence in the parent material or its extent of weathering. Sverdrup and Warfvinge (1995) stated that it is their experience that epidote is present in very many locations, but almost always in small amounts. However, evidence favoring the incorporation of epidote weathering into models of weathering has been reported from selected localities. Schroeder et al. (2000) reported epidote to be dissolved completely in the A horizon of a Georgia Piedmont soil, and Braun and Pagel (1994) found epidote to be destroyed within the first stages of syenite weathering in southwest Cameroon. Recently, Oliva et al. (2004) included epidote in a suite of trace calcic phases that account for more than 80% of the net export of Ca from the Estibère watershed in the French Pyrenees.

The most common reason to invoke epidote dissolution in weathering studies is to overcome the "calcium problem." Bowser and Jones (1993) introduced the term "calcium problem" to refer to the observation that solute analyses of many streams draining small watersheds underlain by crystalline silicate bedrock often contain Ca/Na ratios higher than can be predicted by congruent dissolution of plagioclase feldspar. In silicate-dominated natural hydrologic systems, plagioclase dissolution is the most important weathering reaction (Bowser and Jones 1993, 2002; Drever 1997a; Jacobson et al. 2003), and the calcium problem has become an essential part of weathering studies

* Current address: Department of Earth Sciences, Millersville University, P.O. Box 1002, Millersville, PA 17551-0302. E-mail: Jason.Price@millersville.edu.

0003-004X/05/0001–101$05.00/DOI:10.2138/am.2005.1444

(Drever 1997a). A fundamental explanation commonly offered to explain the calcium problem is that there is an additional, unrecognized, source of Ca (Drever 1997a; Bowser and Jones 2002) such as calcite (e.g., Velbel 1992; Blum et al. 1998; White et al. 1999; Taylor et al. 2000a,b), apatite (e.g., Aubert et al. 2001, 2002; Blum et al. 2002; Oliva et al. 2004), and/or Ca-rich silicate minerals that typically occur in minor to trace abundances (e.g., epidote-group minerals; Oliva et al. 2004).

Epidote-group minerals contain independent SiO_4 tetraheda and Si_2O_7 groups. Their structure is based on chains of edge-sharing octahedra of two types; (1) a single chain of M2 octahedra, and (2) a multiple or zig-zag chain composed of a chain of M1 octahedra with peripheral M3 octahedra attached on alternate sides along its length (Dollase 1971; Deer et al. 1986). The chains of octahedra are parallel to **b**, and are cross-linked in the **c**-axis direction by groups of single SiO_4 tetrahedra and Si_2O_7 dimers. The large cavities that remain between the chains and cross-links host the A1 and A2 cations in nine and tenfold coordination, respectively (Dollase 1971; Deer et al. 1986). Both epidote and allanite are monoclinic with $P2_1/m$ symmetry (Mitchell 1966; Dollase 1971; Deer et al. 1986).

Among epidote-group minerals, the only variations in cation occupancy involve the A2, M1, and M3 sites. The M2 octahedra contain only Al, with the M3 site containing a larger fraction of the non-Al cations (Dollase 1971). The non-random distribution of the cations in the three octahedral sites likely reflects the preference of Al to coordinate with hydroxyls in M2, and the preference of the transition metals for the larger and more distorted M3 site (Dollase 1971). In epidote, the A sites are entirely occupied by Ca, whereas in allanite, Ca is partially replaced by other divalent ions, such as Sr and Pb, or by the rare-earth elements (REE) (Dollase 1971). Substitution is non-uniform between the A sites, such that all of the ions replacing Ca are found only in the A2 site (Dollase 1971). This phenomenon is explained by the larger A2 site hosting cations that are larger than Ca (Dollase 1971). The A2 site is tenfold coordinated, except when occupied by lanthanides in which case it becomes 11-fold coordinated (Dollase 1971). Strens (1966) noted that the replacement of Ca by trivalent cations in allanite strengthens the bonding across (001) and reduces the tendency for {001} cleavage to occur. The reorganization of the epidote structure due to cationic substitutions is largely described by major rotations and minor translations of polyhedra (Dollase 1971).

Allanite is the epidote-group mineral characterized by an abundance of REE in A2 sites, especially Ce (Frondel 1964; Mitchell 1966; Burt 1989; Hermann 2002; Ercit 2002). Ercit (2002) provided the following general formula for allanite:

$$Ca(REE,Y)(Al,Fe^{2+},Fe^{3+})_3(Si_2O_7)(SiO_4)O(OH)$$

The chemical relationship between allanite and other epidotes may be expressed as:

$$Ca^{2+} + Fe^{3+} = REE^{3+} + Fe^{2+}.$$

Allanite is the only epidote-group mineral in which Fe^{2+} is an essential constituent (Deer et al. 1986).

Allanite commonly occurs in the metamict state due to the destruction of the crystal structure by α-particle bombardment emitted by U and/or Th contained in the A2 sites (Wilson 1966; Bromley 1964; Mitchell 1966; Ewing 1976; Ewing and Haaker 1981; Deer et al. 1986; Peng and Ruan 1986; Palmquist 1990; Janeczek and Eby 1993; Ercit 2002). The degree of metamictization is influenced by the age of the allanite and the amount of U and Th present, not by any variation of the REE (Hata 1939; Frondel 1964). The presence of radioactive elements also makes allanite useful for geochronology (e.g., Wilson 1966; Poitrasson et al. 1998). Metamictization lowers the persistence of allanite, making it more susceptible to alteration, including weathering (Deer et al. 1986; Ercit 2002). Metamictization of allanite has been reported to be capable of causing the release of REE from the crystal structure (Peng and Ruan 1986).

In thin section, non-metamict allanites are distinguished by their brownish color, whereas metamict grains behave isotropically and contain anastomosing fractures (Bromley 1964; Deer et al. 1986). Metamict minerals also may not conform to an ideal structural formula (Deer et al. 1986; Ercit 2002).

Perhaps the earliest formal description of the weathering of allanite is that of Watson (1917). He examined an extensive collection of fresh and weathered allanite samples collected from pegmatites in the Atlantic states. All of these weathered allanite samples contained a "...usual reddish brown alteration product from weathering" Watson (1917, p. 469) was able to conclude that the reddish-brown weathered product of allanite was composed of varying amounts of Si, Al, Fe^{3+}, Ce, and H_2O. Furthermore, he noted that in several cases, all of the REE (except Ce) present in the fresh mineral were completely lost from the weathering crust (Watson 1917). Hata (1939) arrived at identical conclusions from studying allanite from the granite region of the Abukama Range, Japan, and also determined that allanite weathering started with the dissolution of the REE.

In his classic work on chemical weathering, Goldich (1938) reported that the allanite found in the Morton Gneiss of Minnesota was one of the least persistent minerals during weathering, and categorized it with the other relatively weatherable minerals plagioclase, epidote, hornblende, titanite, and apatite. Similarly, Ramspott (1965) reported that accessory allanite weathers very rapidly in the Elberton Granite of Georgia, although epidote rims on allanite are not discernibly weathered at the thin section scale. In the Elberton Granite, allanite is present as both unaltered single grains, as well as colorless, nearly isotropic, metamict grains (Ramspott 1965).

Delvigne (1998; his Plates 231 and 232, p. 185) provided a thin section photomicrograph of a metamict allanite that was completely weathered and pseudomorphically replaced by poorly crystalline saponite. The pseudomorph is irregularly surrounded by an incomplete rim of skeletal primary epidote. Delvigne (1998) also noted that the only other mineral observed weathering in same thin section as the allanite was biotite, which is only partially weathered to saponite.

The release of REE during rapid weathering of allanite also has been reported in more recent literature (e.g., Meintzer 1981; Banfield and Eggleton 1989; Braun et al. 1993; Braun and Pagel 1994; Harlavan and Erel 2002). At least 70% of the light REE in a granitic rock may be contained in the accessory minerals allanite, apatite, titanite, and epidote (Gromet and Silver 1983;

Braun et al. 1993; Braun and Pagel 1994); for subducted eclogites, Hermann (2002) found that over 90% of bulk-rock light REE may be incorporated into accessory allanite.

Rare-earth elements are relatively mobile during weathering, as they are not contained in secondary minerals that remain stable during progressive (low pH) weathering (e.g., Banfield and Eggleton 1989; Braun et al. 1990, 1993, 1998 and references therein; van der Weijden and van der Weijden 1995; Cotten et al. 1995; Koppi et al. 1996; Gavshin et al. 1997; Nesbitt and Markovics 1997; Aubert et al. 2001; Patino et al. 2003). The only exception is Ce^{3+}, which oxidizes to Ce^{4+} in the weathering environment and precipitates as cerianite (CeO_2). In contrast, REE released from allanite in hydrothermal systems may have mobility limited to scales of a few to tens of micrometers (e.g., Wood and Ricketts 2000). Wood and Ricketts (2000) found that allanite of the Eocene Casto granite of Idaho released REE during interaction with F-rich hydrothermal solutions, but the REE were rapidly fixed in monazite before being transported any significant distance.

At the Coweeta Hydrologic Laboratory located in western North Carolina (Fig. 1), allanite has been found to be the dominant epidote-group mineral present and is highly weatherable. Epidote is much less abundant and relatively unweatherable, persisting into the solum with only minor evidence of weathering. However, for the lithostratigraphic units at Coweeta, epidote and allanite are typically identical petrographically, and are only distinguished by trace-element analyses. It is allanite, rather than epidote, that provides a previously unrecognized Ca source to Coweeta regolith pore waters.

GEOLOGICAL SETTING

The study area is the U.S. Forest Service Coweeta Hydrologic Laboratory located in the southeastern Blue Ridge Province of western North Carolina (Fig. 1). Coweeta is located approximately 15 km southwest of Franklin, North Carolina, and about 3 km north of the Georgia state line.

The Coweeta Basin is underlain by complexly folded, thrust-faulted, and amphibolite-facies (staurolite-kyanite zone) metasediments of the Coweeta Group (mid-Ordovician; Miller et al. 2000) and the Otto Formation (Upper Precambrian; Hatcher 1980, 1988). The Coweeta Group may be subdivided into three lithostratigraphic units. The basal Persimmon Creek Gneiss is dominantly a massive quartz diorite orthogneiss with interlayers of metasandstone, quartz-feldspar gneiss, and pelitic schist (Hatcher 1980). The overlying Coleman River Formation is characterized by metasandstone and quartz-feldspar gneiss with lesser pelitic schist and calc-silicate quartzite. The Coleman River Formation is overlain by the Ridgepole Mountain Formation; a mineralogically more mature coarse biotite-garnet schist, pelitic schist, metaorthoquartzite, garnetiferous metasandstone, and muscovite-chlorite quartzite (Hatcher 1980). In contrast to the maturity of the Coweeta Group protolith sediments (e.g., arkoses and quartz arenites), the Otto Formation is derived from sedimentary protoliths of low compositional maturity (e.g., graywackes) and comprises a sequence of metasandstones that are feldspar- and biotite-rich, and are interlayered with mafic volcanics and aluminous schists (Hatcher 1988). The Otto Formation is predominantly biotite paragneiss and biotite schist (Hatcher

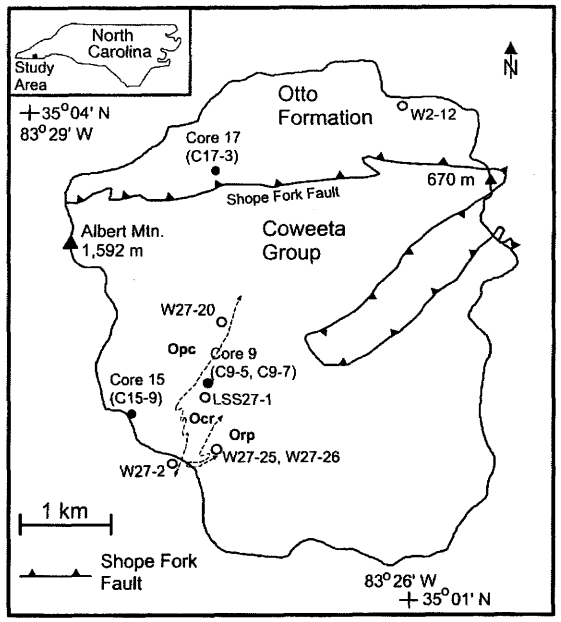

FIGURE 1. Map of Coweeta Hydrologic Laboratory showing bedrock geology, and core and sample locations. Lithostratigraphic units of the Coweeta Group are: Opc = Persimmon Creek Gneiss, Ocr = Coleman River Formation, and Orp = Ridgepole Mountain Formation.

1980). Coweeta Group and Otto Formation rocks are juxtaposed as a result of thrusting of the premetamorphic Shope Fork Fault (Hatcher 1988; Fig. 1). The eastern Blue Ridge Province has, however, been affected by all the major tectonic events that shaped the southern Appalachian orogen (Miller et al. 2000).

Saprolite mantles the landscape at Coweeta, although bedrock may crop out locally, especially near ridge crests. Saprolite is an isovolumetric residuum of chemical weathering, in which the altered mineralogy, petrography, and structural fabric of the saprolite reflect the original crystalline rock types (Mills et al. 1987; Velbel 1990). The average weathering profile (saprolite and soil) at Coweeta is approximately 6 m thick (Berry 1976; Yeakley et al. 1998). The saprolite at Coweeta is not an ancient, relict, deep weathering profile, as evidenced by its great thickness (up to 18 m; Berry 1976; Ciampone 1995) despite residing on very steep slopes (average slope of approximately 45%/23°; Velbel 1985). On such steep slopes, ancient weathering profiles most likely would have succumbed to mass wasting and not have survived to the present. The soil, mostly Ultisols and Inceptisols (Velbel 1988), comprises the uppermost 30 cm of the profile and is the friable material in which parent rock structure and fabric have been destroyed by mass-wasting, root throw, soil infauna, etc. (Velbel 1985).

METHODS

Petrography

Thin sections of bedrock, soil, and saprolite were prepared by standard methods. Bedrock samples were obtained by Berry (1976) during a regolith coring investigation (see Fig. 1 for core locations). Due to the friable nature of the saprolite and soil collected by the authors, clear epoxy was used to vacuum impregnate samples that had been collected in chrome tubes. Grain mounts were also prepared for soil samples collected by the Coweeta staff.

Point counting utilized standard methods, and was completed using bedrock samples of Berry (1976). A minimum of 500 points per thin section were counted.

Bulk major-element oxide analyses

Berry (1976) provided bulk major-element oxide chemical data of the bedrock samples collected during a coring investigation. Core 17 sampled Otto Formation bedrock, Core 9 sampled bedrock of the Coleman River Formation of the Coweeta Group, and Core 15 sampled bedrock of the Persimmon Creek Gneiss of the Coweeta Group (Fig. 1). Berry (1976) sampled the bedrock by diamond-drilling into the unweathered rock. Major-element oxide analyses were performed by atomic absorption methods at the University of Georgia.

Scanning electron microscopy: (SEM) and back-scattered electron (BSE) imaging

Polished thin sections and SEM stubs of Coweeta bedrock and regolith were prepared for examination by SEM and analyzed by energy dispersive X-ray spectroscopy (EDS) for elemental composition. SEM stubs were gold-coated, and thin sections were either carbon- or gold-coated. Gold-coating of thin sections was often necessary because carbon-coating did not always provide adequate conductivity to prevent sample charging. Imaging and analyses were performed at Michigan State University's Center for Advanced Microscopy (CAM) using a JEOL JSM-35CF SEM with EDS and BSE capabilities.

Electron microprobe phase analyses (EMPA)

Electron microprobe analyses of minerals in thin sections of Coweeta bedrock were obtained at the University of Michigan's Electron Microbeam Analysis Laboratory (EMAL), using a wavelength-dispersive Cameca SX 100 electron microprobe analyzer. Accelerating voltage and beam current were 15 keV and 10 nA, respectively, and a beam diameter of 2 μm was used. Calibration standards for Na, Si, Al, Mg, Fe, Mn, Ti, Ca, and K were respectively albite (natural Tiburon), tanzanite (natural), andalusite (natural), enstatite (synthetic), ferrosilite (synthetic), rhodonite (natural Broken Hill), geikielite (natural), tanzanite (natural), and adularia (natural St. Gothard).

Allanite and epidote formulae calculated from the EMPA data assume stoichiometry. True structural formulae of allanite can only be calculated for non-metamict samples (Ercit 2002), and structural formulae for any mineral can only be calculated when the EMPA data contain both FeO and Fe_2O_3. By analogy with allanite and epidote compositions reported by Deer et al. (1986), the calculated formulae for Coweeta allanite likely contain ferrous and ferric iron in approximately equal proportions, and the Coweeta epidote has been assigned all Fe^{3+}.

Rare-earth element analyses by inductively coupled plasma mass spectrometry (ICP-MS)

Rare-earth element analyses of allanite and epidote were performed on a Micromass Inductively Coupled Plasma Mass Spectrometer (ICP-MS) at Michigan State University. The REE included in this study are lanthanum (^{139}La), cerium (^{140}Ce), neodymium (^{146}Nd), gadolinium (^{158}Gd), dysprosium (^{163}Dy), and ytterbium (^{173}Yb). These six REE were selected based on their relatively high abundance (above background) in a scan of Coweeta stream waters.

Laser ablation ICP-MS (LA-ICP-MS) analyses on grains in thin section were performed using a Cetac LSX 200$^+$ laser ablation system. LA-ICP-MS provides high-resolution sampling capabilities and multi-element high sensitivity (Fryer et al 1995; Neal et al. 1995). The beam size was 25 μm (using a UV, 266 nm beam), and the pulse rate was 20 Hz. LA-ICP-MS and EMPA analyses spots were adjacent to one another, and Ca was used as the internal standard for all laser ablation analyses (Fryer et al. 1995; Longerich et al. 1996). NIST 612 glass was used as a calibration standard and results were obtained in μg/g. LA-ICP-MS detection limits are influenced by instrument operating conditions, scanning parameters, mass of material ablated, and the homogeneity of the mineral at the sample scale (Jackson et al. 1992; Perkins et al. 1993; Jenner et al. 1993; Jeffries et al. 1995). Detection limits (ppb/element wt% oxide) for La/La_2O_3, Ce/Ce_2O_3, Nd/Nd_2O_3, Gd/Gd_2O_3, Dy/Dy_2O_3, and Yb/Yb_2O_3 are 5.2/0.00061, 29/0.0034, 11/0.0012, 4.7/0.00054, 8.1/0.00093, and 11/0.0012, respectively. Calculation of detection limits followed methods of Norman et al. (1996). Precision of LA-ICP-MS analyses is 7%. For comparison with major-element analyses, LA-ICP-MS data are reported as wt% oxide. When REE data are normalized to chondrite values, the REE abundances of Sun and McDonough (1989) were used.

Results

The modal mineralogies for Otto Formation and Coweeta Group bedrock at Coweeta are presented in Table 1. The bulk major-element oxide analyses of bedrock samples completed by Berry (1976) are provided in Table 2. Note that Berry recalculated all his analyses to 100%.

The combined EMPA and LA-ICP-MS analyses for allanite (and epidote in some cases) grain cores and rims yield relatively low totals (Table 3). Deer et al. (1986) reported allanite analyses that sum to near 100%, but include analyses for structural and non-structural water, both FeO and Fe_2O_3, UO_2, ThO_2, and additional REE not included in the analyses of this study. If UO_2, ThO_2, and H_2O are subtracted from the allanite totals reported by Deer et al. (1986), then totals may be as low as 90%. However, the allanite totals reported in Table 3 are still typically below 90%, and as low as approximately 70% (Otto Formation allanite cores, Table 3). Analytical totals below approximately 96% (including calculated H_2O) are evidence of metamictization (Ercit 2002). Such low EMPA totals do not prevent calculation of a stoichiometric formula, although Si contents greater than 3.09 atoms per formula unit have been found for the Otto Formation allanite (Table 4). Such excess Si contents are indicative of metamictization (Ercit 2002). The CaO concentrations in allanite (Table 3) are well within the range reported by Deer et al. (1986), despite the low totals. As Ca is located in interchain tunnels in epidote-group minerals, it would be most readily lost during alteration and metamictization (e.g., Peng and Ruan 1986; Barman et al. 1992; Varadachari et al. 1992; Kalinowski et al. 1998). The stoichiometric formulae for Coweeta epidote-group minerals are contained in Table 4.

Petrography, electron microscopy, and composition

The importance of allanite as a Ca reservoir in bedrock is presented in Table 5. Average Coweeta garnet and plagioclase compositions and the Coleman River Formation allanite composition are used, along with the average modal abundances of each mineral. The composition of Coleman River Formation allanite is included because it contains the lowest formula proportion of Ca of all the Coweeta allanites (Table 4), thereby providing calculation of a minimum Ca contribution from allanite. Note from Table 5 that, despite constituting on average <1% of the bedrock by volume, allanite may contain a minimum of 25% of the bedrock Ca. Furthermore, garnet contains only 5% of the total Ca in the Coweeta bedrock, with plagioclase containing 70% of the total Ca.

Chemically, the distinction between isostructural allanite and epidote is in the substitution of Ce for Ca in A2 sites (e.g., Frondel 1964; Dollase 1971; Deer et al. 1986; Janeczek and Eby

Table 1. Modal mineralogies for Ca-bearing phases of the Otto Formation and Coweeta Group bedrock

Sample	Bedrock*	Depth (m)	Plagioclase (%)	Garnet (%)	Allanite (%)
C17-3	OF	1.3	16.2	0.7	1.4
C9-5	CRF	6.3	9.9	2.0	0.8
C9-7	CRF	11.3	16.1	2.2	0.5
C15-9	PCG	11.6	17.1	0.0	0.7
Mean			14.8	1.2	0.9

* OF = Otto Formation; CRF = Coleman River Formation; PCG = Persimmon Creek Gneiss.

TABLE 2. Chemical analyses of Otto Formation and Coweeta Group bedrock (data from Berry 1976)

			Weight Percent Oxide											
Sample	Bedrock*	Depth (m)	SiO_2	Al_2O_3	Fe_2O_3	MgO	CaO	Na_2O	K_2O	TiO_2	P_2O_5	MnO	LOI	Total
C17-3	OF	8.7	71.13	12.66	4.92	1.96	3.17	2.47	1.43	0.88	0.17	0.04	1.17	100.00
C9-5	CRF	6.3	73.85	12.27	4.89	1.97	1.11	0.74	1.61	1.95	0.24	0.03	1.34	100.00
C9-7	CRF	11.3	72.04	12.18	5.34	1.73	2.83	2.19	1.28	1.22	0.10	0.02	1.07	100.00
C15-9	PCG	12.8	64.88	16.10	6.65	1.58	2.00	2.04	3.59	1.11	0.13	0.04	1.88	100.00

* OF = Otto Formation; CRF = Coleman River Formation; PCG = Persimmon Creek Gneiss.

TABLE 3. Combined mean EMPA and LA-ICP-MS data for epidote and allanite grain cores and rims from the Coweeta Hydrologic Laboratory

	Otto Formation		Persimmon Creek Gneiss			Coleman River Formation		Ridgepole Mountain Formation			
	Allanite		Allanite	Epidote		Allanite		Allanite		Epidote	
	Core	Rim	Core	Core	Rim	Core	Rim	Core	Rim	Core	Rim
n	2	2	1	1	3	5	4	3	2	2	3
SiO_2	31.72	34.36	37.48	37.12	38.04	32.90	34.15	33.46	33.91	36.64	37.84
TiO_2	0.04	0.05	0.08	0.15	0.13	0.06	0.07	1.06	0.58	0.08	0.06
Al_2O_3	17.60	21.82	24.65	24.07	25.69	20.54	21.14	20.47	20.57	22.77	26.51
FeO*	4.80	6.80	7.89	6.96	8.02	6.69	7.68	7.78	7.32	8.14	6.57
MgO	0.64	0.25	0.02	0.37	0.38	0.13	0.96	0.34	BDL	0.48	0.52
MnO	0.17	0.21	0.24	0.23	0.18	0.17	0.17	0.16	0.16	0.20	0.26
CaO	12.89	17.95	21.82	19.89	22.83	15.16	16.57	15.63	16.71	20.02	21.97
Na_2O	1.14	0.54	0.28	0.39	0.09	0.54	0.18	0.40	0.52	0.24	0.07
K_2O	0.02	0.05	0.07	0.02	0.04	0.08	0.05	0.22	0.13	0.01	BDL
La_2O_3	0.14	0.16	0.019	0.0079	0.0062	0.38	0.26	0.20	0.55	0.00033	0.00069
Ce_2O_3	0.28	0.31	0.055	0.019	0.0077	0.56	0.43	0.35	0.94	BDL	BDL
Nd_2O_3	0.18	0.20	0.051	0.013	0.0025	0.37	0.26	0.20	0.50	0.00060	0.00051
Gd_2O_3	0.034	0.039	0.012	0.0034	BDL	0.095	0.060	0.043	0.087	BDL	BDL
Dy_2O_3	0.018	0.030	0.0091	0.0036	BDL	0.093	0.059	0.020	0.040	BDL	BDL
Yb_2O_3	0.014	0.021	0.0040	0.0017	BDL	0.029	0.022	0.0061	0.015	BDL	BDL
Total	69.67	82.77	92.68	89.24	95.41	77.81	82.05	80.35	82.03	88.57	93.79

Note: BDL = Below detection limits.

TABLE 4. Stoichiometric formulae for Coweeta epidote-group minerals

Mineral	Lithostratigraphic Unit	n	Stoichiometric Formula
Allanite	Otto Formation	4	$(Ca_{1.58}Mn_{0.02}Na_{0.16}La_{0.0053}Ce_{0.010}Nd_{0.0066}Gd_{0.0011}Dy_{0.00073}Yb_{0.00050})Fe_{0.46}Mg_{0.06}Al_{2.22}Si_{3.16}O_{12}OH$
Allanite	Persimmon Creek Gneiss	1	$(Ca_{1.86}Mn_{0.02}Na_{0.04}K_{0.01}La_{0.00056}Ce_{0.0016}Nd_{0.0014}Gd_{0.00031}Dy_{0.00023}Yb_{0.000096})Fe_{0.53}Al_{2.31}Si_{2.98}O_{12}OH$
Allanite	Coleman River Formation	9	$(Ca_{1.55}Mn_{0.01}Na_{0.08}K_{0.01}La_{0.011}Ce_{0.017}Nd_{0.011}Gd_{0.0024}Dy_{0.0023}Yb_{0.00073})Fe_{0.55}Mg_{0.09}Al_{2.25}Si_{3.08}O_{12}OH$
Allanite	Ridgepole Mountain Formation	5	$(Ca_{1.57}Mn_{0.01}Na_{0.08}K_{0.02}La_{0.011}Ce_{0.020}Nd_{0.010}Gd_{0.0018}Dy_{0.00082}Yb_{0.00027})Ti_{0.06}Fe_{0.57}Mg_{0.03}Al_{2.20}Si_{3.07}O_{12}OH$
Epidote	Persimmon Creek Gneiss	4	$(Ca_{1.83}Mn_{0.01}Na_{0.3}La_{0.00025}Ce_{0.00040}Nd_{0.00019}Gd_{0.000087}Dy_{0.000089}Yb_{0.000039})Ti_{0.01}Fe_{0.50}Mg_{0.04}Al_{2.31}Si_{2.93}O_{12}OH$
Epidote	Ridgepole Mountain Formation	5	$(Ca_{1.79}Mn_{0.02}Na_{0.02}La_{0.000027}Nd_{0.000039})Fe_{0.48}Mg_{0.06}Al_{2.33}Si_{2.95}O_{12}OH$

TABLE 5. Assessment of the minimum allanite contribution to bedrock Ca at Coweeta Hydrologic Laboratory

	Allanite	Garnet	Plagioclase
Specific Gravity (g cm^{-3})	3.9*	4.32*	2.66*
Formula	$(Ca_{1.55}Mn_{0.01}Na_{0.08}K_{0.01}Ce_{0.017})$-$Fe_{0.55}Mg_{0.09}Al_{2.25}Si_{3.08}O_{12}OH$†	$Ca_{0.31}Mg_{0.33}Mn_{0.41}Fe_{1.94}Al_2Si_3O_{12}$†	$Ca_{0.30}Na_{0.70}Al_{1.30}Si_{2.70}O_8$†
Formula Weight	456.4	481.6	267.0
Modal Abundance (%)	0.9	1.2	14.8
Ca (mol m^{-3})	154	34	442
Ca Fraction in Rock (%)	25	5	70

* Data from Klein and Hurlbut (1999).

† Stoichiometric formulae based on an average of 9 EMPA analyses of Coleman River Formation allanite (Table 3), 16 EMPA analyses for garnet, and 13 EMPA analyses for plagioclase.

1993; Klein and Hurlbut 1999; Ercit 2002). However, appreciable values of Ce have been reported for epidote (e.g., Grauch 1989), thereby obscuring the distinction between epidote and allanite (Ercit 2002). A complete solid solution series may exist between epidote and allanite (Frondel 1964). In a review of REE abundances in epidote-group minerals, Grauch (1989) reported epidote/chondrite La ratios as being less than approximately 1000, whereas the same ratios for allanite are approximately 100 000 or greater. However, many of the epidote-group minerals at Coweeta fall in between these two values (Fig. 2), and may be termed either high-REE epidote or low-REE allanite. Any epidote-group mineral at Coweeta that yields a mineral/chondrite La ratio of the greater than 1000 will be referred to herein as allanite. It should be recognized, however, that the Coweeta allanite is relatively low in REE (Fig. 2) when compared with published data for many allanites (Deer et al. 1986; Grauch 1989). In thin section, the unweathered allanite grains typically have optical properties that resemble epidote more so than allanite (e.g., optically anisotropic in thin section; Fig. 3). Making this distinction is important, because at Coweeta, the bedrock contains both allanite and epidote that are indistinguishable in thin section when unweathered (Fig. 3). However, the allanite is far more abundant and dissolves rapidly below the weathering front. In contrast, epidote is less abundant and persists into the solum with only minimal evidence of weathering (Fig. 4). These observations underscore the importance of analytical data (e.g., EDS, ICP-MS) when conducting studies that include the weathering of epidote-group minerals, and may be offered to ex-

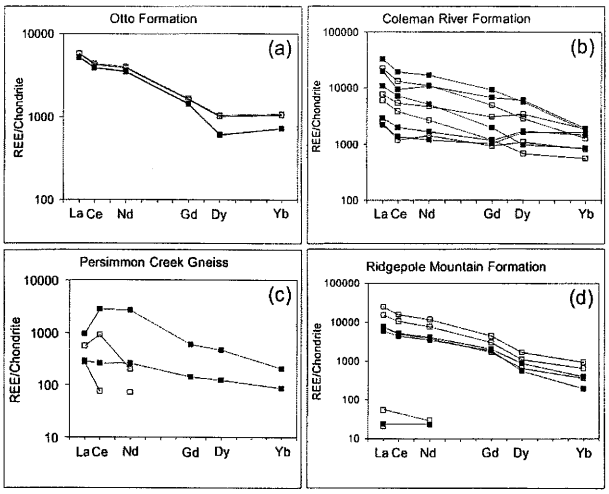

FIGURE 2. Chondrite normalized REE patterns of epidote-group mineral cores (closed symbols) and rims (open symbols) from the lithostratigraphic units at Coweeta Hydrologic Laboratory; (a) Otto Formation, (b) Coleman River Formation, (c) Persimmon Creek Gneiss, and (d) Ridgepole Mountain Formation.

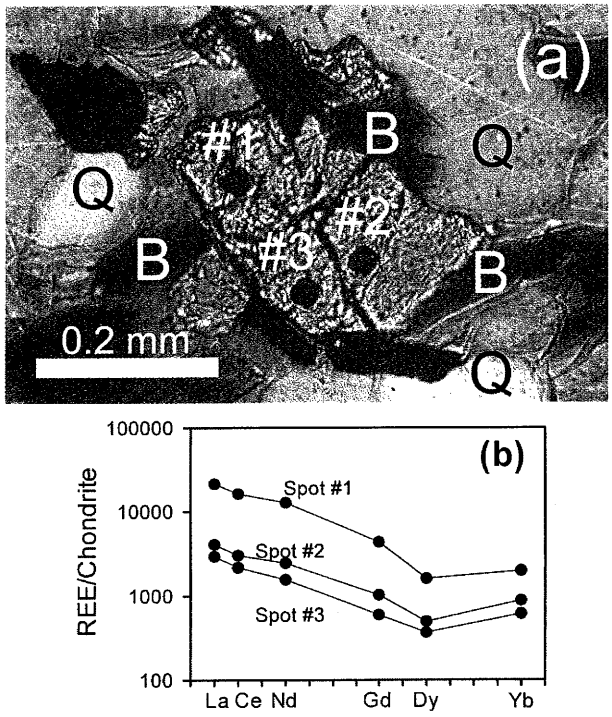

FIGURE 3. Photomicrograph and REE patterns of an epidote-group mineral at Coweeta. This grain has the optical properties of an epidote (**a**), but the REE content of an allanite (**b**). The three dark circles on grain are laser ablation pits and correspond to the REE plot (b). Image (a) is plane-polarized light, with B = biotite and Q = quartz. Sample C17-3 from the Otto Formation.

plain why "epidote" has been reported to be destroyed within the first stages of weathering (e.g., Braun and Pagel 1994) – highly weatherable allanite may be misidentified as epidote by many conventional methods.

Figure 2 illustrates REE patterns of both cores and rims of epidote-group minerals. Only in the Persimmon Creek Gneiss is there a significant distinction between the REE content of cores and rims. The lack of distinction between the REE content of allanite cores and rims using LA-ICP-MS may be a result of the diameter of the beam being similar in size to the thin allanite rims (approximately 25 μm; Fig. 5), compounded by noting that the core-rim boundary is not always evident (Fig. 3), if a rim is present at all. In general, the most significant difference between the cores and rims of allanite grains at Coweeta is that the cores weather preferentially to the rims. However, both rims and cores weather relatively rapidly with respect to all other minerals present in the rock.

Although allanite grains, either cores or rims, at Coweeta are generally not sufficiently metamict to be optically isotropic, allanite grains are commonly associated with pleochroic haloes in adjacent biotite when observed petrographically. However, neither U nor Th has been detected using EDS, even in grains that are petrographically isotropic (Fig. 6). The lack of detection of U and Th indicates concentrations at levels below the detection limits of EDS; perhaps U and Th were mobilized from the grains, and/or they have decayed away. Allanite grains with isotropic cores and fractures occur only in the Persimmon Creek Gneiss, (Fig. 6a). Grains exhibiting such extensive metamictization are uncommon in the study area. These same grains yield microprobe analyses with very low totals (<65 wt%) that, like many metamict minerals, do not permit recalculation of a reasonable structural formula (Deer et al. 1986; Ercit 2002).

The allanite cores (Fig. 6) in the metasedimentary rocks at Coweeta are of detrital origin (Hatcher 1980), so they have already survived one pass through the sedimentary cycle. The rims on the cores likely formed during the most recent episode of metamorphism (Taconic Orogeny), and thus are younger than the cores. The allanite cores may weather preferentially to the rims because they are older, and likely more metamict, than the rims (Frondel 1964), rather than containing more REE (Hata 1939; Frondel 1964). If so, then the temperature of the amphibolite-facies metamorphism in the study area during the Taconian Orogeny was not sufficiently high (<600 °C; e.g., Frondel 1964, Janeczek and Eby 1993) to anneal the detrital allanite. This is consistent with the bedrock of Coweeta having been subjected to lower to middle amphibolite-facies metamorphic conditions (Hatcher 1988). Nonetheless, with the exception of uncommon allanite grains in the Persimmon Creek Gneiss, allanite cores and rims are usually anisotropic in thin section (Fig. 6).

Both the Otto Formation and Coweeta Group rocks contain epidote grains that persist in the regolith (Fig. 4). For example, based on REE contents, the Persimmon Creek Gneiss and Ridgepole Mountain Formation contain both epidote and allanite (Fig. 2). Microscopically, the epidote typically does not contain an allanite core (with the exception of the Persimmon Creek Gneiss; Figs. 2 and 6), although an epidote grain with a thin (~ 3 μm) rim that is also epidote has been noted (Fig. 4a). The persistence of Coweeta epidote into the solum (Fig. 4) supports the relative resistance of epidote to weathering (e.g., Allen and Hajek 1995; Lång 2000), and demonstrates the danger of invoking epidote weathering without mineralogic observations (e.g., Warfvinge

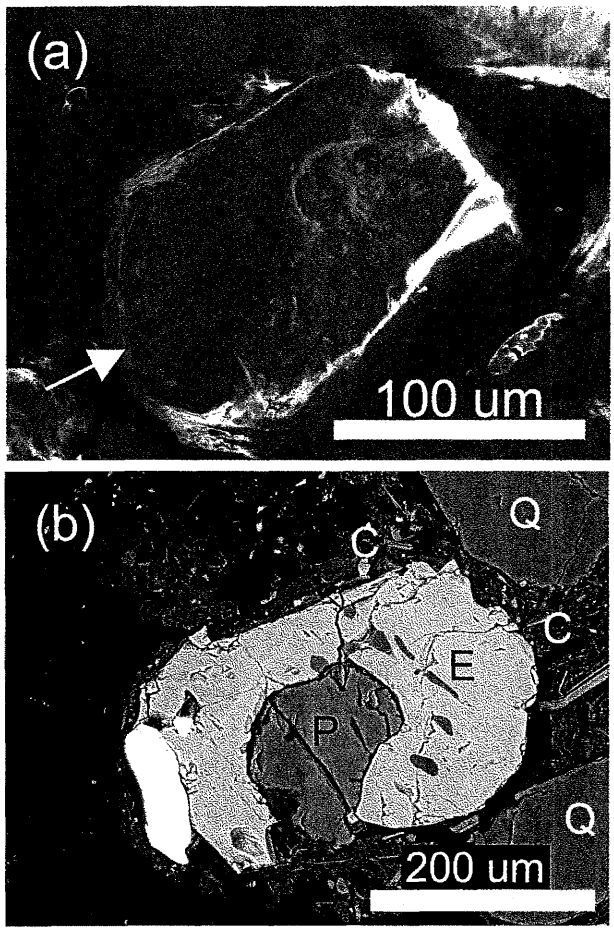

FIGURE 4. Examples of epidote grains found in the solum at Coweeta. Note absence of allanite cores. SEM image of an epidote grain with an epidote rim (arrow) (**a**). BSE image of an epidote (E) grain surrounding a plagioclase (P) grain (**b**). Small dark inclusions in **b** are quartz (Q), and C = clay. Otto Formation B horizon sample W2-12 (**a**), and Coleman River Formation A horizon sample LSS27-1 (**b**).

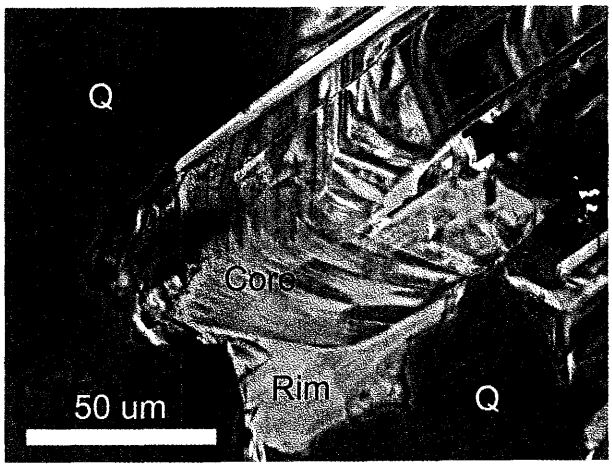

FIGURE 5. BSE image showing an example of a core and rim of an allanite grain at Coweeta; Q = quartz. Coleman River Formation sample C9-7.

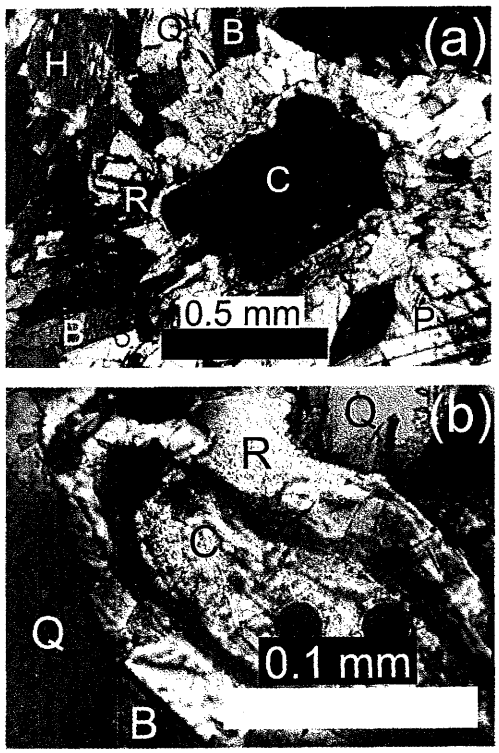

FIGURE 6. Comparison of allanite core (C)-rim (R) combinations; (a) a substantially metamict core that behaves isotropically, and (b) a minimally metamict core. Photomicrograph (a) is thin section W27-20 from the Persimmon Creek Gneiss in crossed-polarized light, and (b) is thin section C17-3 from the Otto Formation in crossed-polarized light. Q = quartz, H = hornblende, B = biotite, and P = plagioclase.

and Sverdrup 1992; Sverdrup and Warfvinge 1993, 1995). However, solum epidote grains at Coweeta often have etch pits (described below). For this reason, observations of epidote and allanite weathering are combined. Because allanite and epidote are isostructural, they provide complementary data on the nature of weathering of epidote-group minerals at Coweeta.

The crystal-chemistry of epidote-group mineral weathering

Allanite weathering at Coweeta is rapid, with complete dissolution occurring below the weathering front and prior to the weathering of any other minerals, except perhaps biotite. Furthermore, both allanite and epidote grains are generally small (<200 μm), anhedral, and present in very low abundances. These factors make separation of epidote-group mineral grains, as well as interpretation of crystal-chemistry, very difficult.

Although obtaining relatively large subhedral to euhedral epidote and allanite grains that may be oriented crystallographically is not possible for Coweeta, evaluating the crystal-chemistry of epidote-group minerals may provide insight into their weathering process. The epidote structure contains continuous chains of AlO_6 and $AlO_4(OH)_2$ octahedra oriented parallel to the b-axis, and cross-linked by SiO_4^{4-} groups and $Si_2O_7^{6-}$ dimers. This cross-linking produces large aligned interchain cavities (the A sites that contain Ca and REE) that form channels parallel to the octahedral chains (Dollase 1971, Deer et al. 1986, Kalinowski et al. 1998).

Crystallographic information may be combined with the results of low-temperature laboratory epidote dissolution experiments (Barman et al. 1992, Varadachari et al. 1992, Kalinowski et al. 1998). Laboratory epidote dissolution experiments have recently been conducted at a range of pH levels, using organic acids (Barman et al. 1992; Varadachari et al. 1992), inorganic acids (Kalinowski et al. 1998), and deionized water (Kalinowski et al. 1998). Despite the variability of experimental methods of these studies, they all agree that the solubilization of cations during epidote dissolution is crystallographically controlled and follows the order Ca > Si > Fe > Al, with the exception of studies that used oxalic, salicylic, or glycine acids (Schalscha et al. 1967; Barman et al. 1992), during which the relative release of Fe and Al was reversed. As stated previously, Hata (1939) determined that allanite weathering started with dissolution of the REE, consistent with the work of Meintzer (1981) on allanite from the Virginia Blue Ridge. The rapid release of Ca from epidote and the REE from allanite is attributed to its being located in the interchain tunnels, outside the octahedral chain (Barman et al. 1992, Kalinowski et al. 1998). The interchain tunnels provide uninhibited access to solvents (Barman et al. 1992), as well as an easy path for hydrated Ca and REE out of the crystal structure (Kalinowski et al. 1998). Kalinowski et al. (1998) also suggested that protonation of the Si-O-Al oxygen atoms in the Si-dimers causes the O atoms in the dimers to become less negative, reducing the attraction to the Ca, and facilitating release of the Ca. The Si-tetrahedra are only present as links between adjacent Al chains and are more readily removed from the structure than the Al located in polymeric chains (Barman et al. 1992). In the experiment of Kalinowski et al. (1998), where deionized water with pH = 5.6 was used as the solvent, which is most similar to natural weathering conditions, the reactor output solutions were saturated with respect to gibbsite, and as a result, no residual surface layer could be calculated for the epidote surface. Based on molar-volume calculations, Velbel (1993) reports that epidote is not likely to form any type of clay protective surface coating.

An image of unweathered allanite is displayed in Figure 7, and, despite evidence of metamictization noted in thin section (i.e., pleochroic haloes in juxtaposed biotite), the basal cleavage is well developed. Two types of etch pits have been found on epidote-group mineral grains from Coweeta and are presented in Figures 8 and 9. The outline of six-sided "negative crystals" may indicate that larger pits form on more easily etched surfaces (Fig. 8). Etch pits with morphology similar to those pictured in Figure 8 have been illustrated and described for feldspars and termed "prismatic" etch pits (e.g., Wilson 1975; Keller 1976, 1978; Berner and Holdren 1977, 1979; Velbel 1986). However, the prismatic etch pits on feldspars noted by these researchers formed by extensive deepening of an etch pit with a relatively small surface expression. That is not believed to be the case for the epidote-group minerals of this study, because no etch pits were found that displayed a small surface opening, but with great visible depth. Smaller, shallow, etch pits are also present on the surfaces of epidote-group minerals at Coweeta (Fig. 9).

The two types of etch pits pictured in Figures 8 and 9 could reflect two different degrees of weathering, with the smaller etch pits reflecting a lesser degree of weathering relative to the larger, negative-crystal etch pits that would form after more advanced weathering. However, this is not believed to be the case for three reasons: (1) no etch pits have been found that may reflect an intermediate stage of weathering between the two types of etch pits pictured; (2) etch pits similar to the smaller etch pits of this study have been noted on minerals very resistant to weathering such as staurolite (Velbel et al. 1996), and negative-crystal etch pits have been noted on relatively weatherable minerals

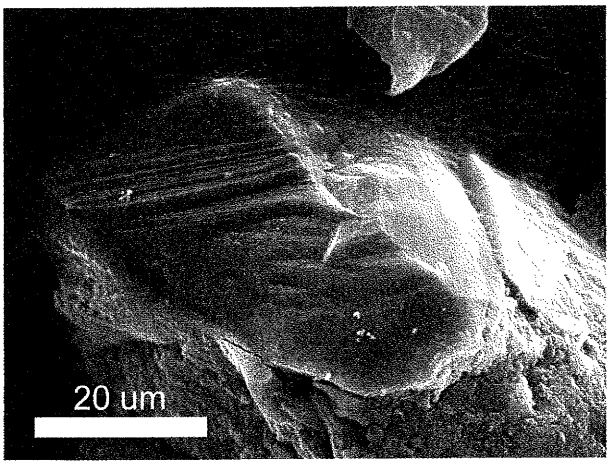

FIGURE 7. SEM image of an unweathered allanite grain. Note perfect basal cleavage. Grain hand picked from Coleman River Formation sample C9-7.

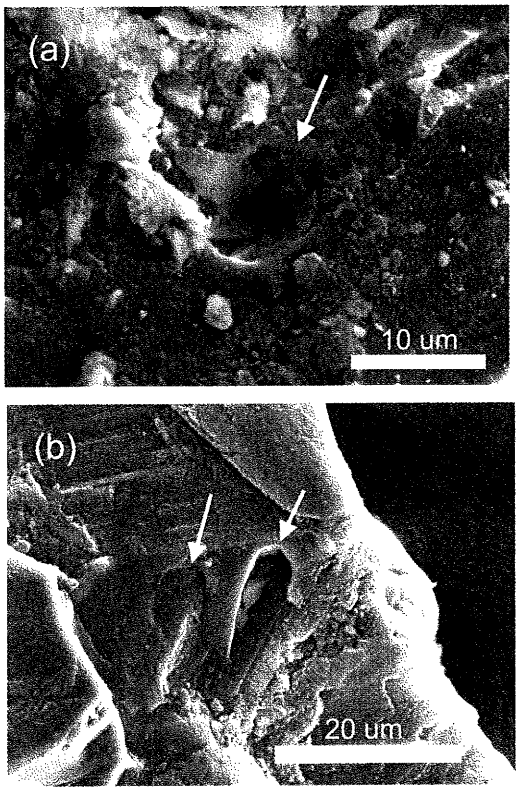

FIGURE 8. Examples of large "negative crystal" etch pits on epidote-group mineral surfaces. Grains are epidote from Otto Formation sample W2-12 (a), and allanite from Coleman River Formation sample C9-7 (b).

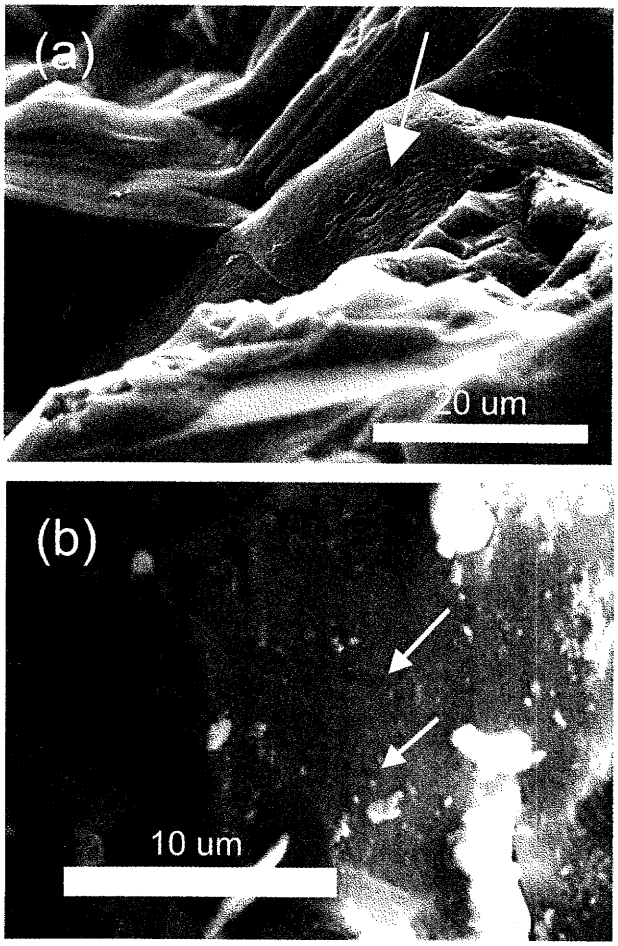

FIGURE 9. Examples of small, shallow etch pits (arrows) on epidote-group mineral surfaces. Note elongation of pits. Grains are allanite from the Coleman River Formation sample C9-7 (a) and, an epidote from Otto Formation sample W2-12 (b).

such as garnet (e.g., Velbel 1984, 1993) and plagioclase (e.g., Berner and Holdren 1977, 1979; Velbel 1983, 1986; Hochella and Banfield 1995); and (3) both types of etch pits have been observed on the same grain, but on different surfaces. Although epidote-group mineral grains cannot easily be oriented permitting the crystal-chemistry of etch pit formation to be determined, etch pits on epidote-group mineral grains do appear to be of two types, each of which is related to a different orientation in the crystal structure.

Etch pit formation should be strongly influenced by the polymeric octahedral chains. The Ca, REE, and Si are the most easily solubilized cations in the epidote-group mineral structure, and the polymeric octahedral chains containing the Al and $Fe^{2+/3+}$ are very resistant to dissolution (Barman et al. 1992; Varadachari et al. 1992; Kalinowski et al. 1998). The nature of etch pit formation on allanite and epidote grains during weathering should reflect these principles. Therefore, the larger etch pits likely deepen parallel to the polymeric octahedral chains and occur on the faces of the (010) pinacoid. In contrast, deepening of the small etch pits is likely impeded by the presence of the polymeric chains. The small etch pits would therefore occur on all faces other than the (010) pinacoid.

Weathering products

Although the allanite grains at Coweeta are very small and difficult to liberate and isolate from the incipiently weathered rock, several remarks about the weathering products of allanite dissolution may be made. Perhaps one of the important aspects of allanite weathering at Coweeta is the absence of weathering products. This differs from the weathering of primary REE-bearing accessory phosphate minerals such as apatite and monazite, which are associated with any of several secondary phosphates such as florencite and rhabdophane (e.g., Banfield and Eggleton 1989; Braun et al. 1998; Aubert et al. 2001). Detailed BSE imaging and X-ray mapping were performed, but no secondary REE-bearing phases were detected. If present at Coweeta, secondary REE-bearing accessory minerals would have to be in extremely low quantities. Figure 10 displays a single allanite grain from the Persimmon Creek Gneiss in which several stages of weathering have been preserved. Points no. 1 and no. 2 in Figure 10 show relatively unweathered high-REE and low-REE allanite, respectively. The low-REE allanite (point no. 2) contains relatively higher Ca than does the high-REE allanite (point no. 1) (Figure 10). Point no. 3 (Fig. 10) is on weathered allanite in which Ca is depleted and Fe is enriched. Nearly complete dissolution of allanite with retention of Fe (goethite) is reflected by point no. 4 (Fig. 10).

There is evidence that carbonate may precipitate during allanite dissolution (Fig. 11). As stated previously, with the exception of biotite, allanite is the first phase to weather at Coweeta, and it completely dissolves below the weathering front. Similar observations at other localities have been made by Goldich (1938) and Delvigne (1998). This incipient stage of weathering is certainly characterized by very low permeabilities and likely a relatively high pH, as allanite hydrolysis is a hydrogen-consuming reaction. Relatively high pH conditions during allanite weathering are supported by the combined observations that Al is mobile at high pH (e.g., Nagy 1995; Drever 1997b; Taylor and Eggleton 2001) and Fe is precipitating (Fig. 10; e.g., Schwertmann and Taylor 1995). That is, no gibbsite or kaolinite has been found associated with weathered allanite grains. Carbonate should be readily leached once continued mineral dissolution creates adequate porosity to change the conditions from those conducive to carbonate precipitation (i.e., relatively high pH and low leaching). In laboratory experiments of epidote dissolution at pH = 10.6, Nickel (1973) found that Ca was not readily released to solution. He invoked carbonate precipitation to explain his observations. SEM images of the suspect carbonate show a spar-like texture (Fig. 11), and EDS spectra indicate the presence of Ca, Fe, and anomalously high C counts.

DISCUSSION

The rate-determining step of the hydrolysis of silicate minerals during chemical weathering is one of the following: (1) transport control in which either transport of solvents to, or products from, the dissolving mineral is rate-limiting; (2) interface control whereby the detachment of ions or molecules

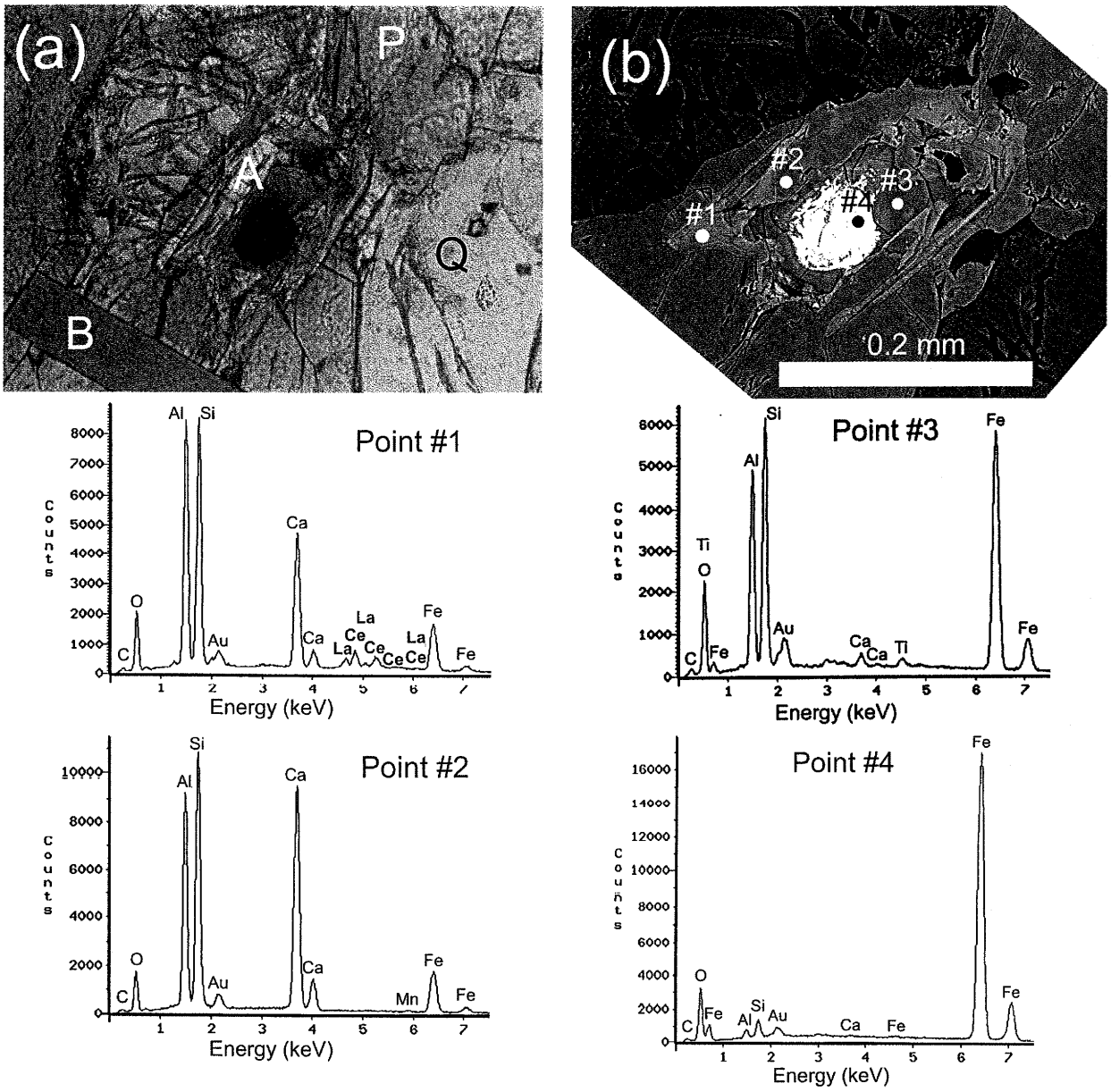

FIGURE 10. Example of the stages of allanite weathering at Coweeta. Image (a) shows an allanite (A) grain in plane-polarized light, and (b) is a BSE image. Sample W27-2 from the Persimmon Creek Gneiss. B = biotite, P = plagioclase, and Q = quartz.

from the mineral surface is rate-limiting; or (3) a combination of transport and interface control (Berner 1978, 1981; Blum and Lasaga 1987; Schott and Petit 1987; Velbel et al. 1996). In pure transport-controlled dissolution, ions are detached so rapidly from the surface of a crystal that they become concentrated in the solution adjacent to the mineral surface (Berner 1978, 1981). As a result, dissolution is regulated by transport of these ions via advection or diffusion away from the mineral surface (Berner 1978, 1981). The surfaces of minerals dissolving by transport control are smooth, rounded, and featureless (Berner 1978, 1981; Velbel et al. 1996). In contrast, during pure interface-controlled dissolution, ion detachment from the mineral surface is so slow that transport of solutes away from the mineral prevents an increase in ion concentration adjacent to the crystal surface (Berner 1978, 1981; Schott and Petit 1987). Under such circumstances, increased advection or diffusion away from the mineral surface has no effect on the dissolution rate (Berner 1978, 1981). Interface-limited mechanisms result in etch pit formation on mineral surfaces, reflecting the site-selective nature of the interfacial reaction (Berner 1978, 1981; Blum and Lasaga 1987; Velbel et al. 1996).

The ubiquity of etch pits on the surfaces of epidote-group minerals collected from Coweeta (Figs. 8 and 9) might indicate that epidote and allanite weathering proceeds by interface-controlled dissolution kinetics, like most silicate minerals (Berner 1978; Lasaga 1984; Schott and Petit 1987; Velbel 1993). This interpretation is consistent with the laboratory-determined activation energy for epidote dissolution being 83 kJ/mol (although

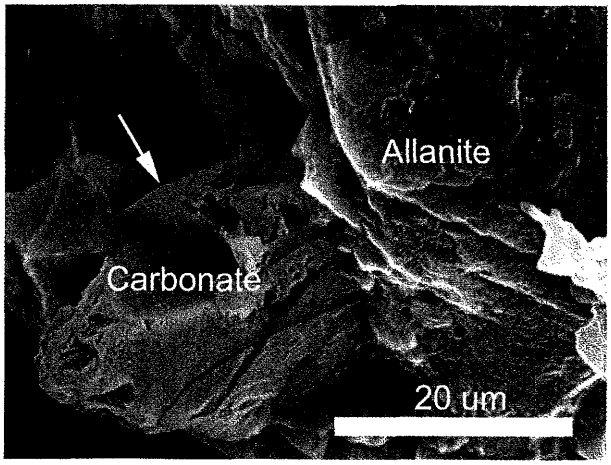

FIGURE 11. Carbonate on the surface of a nearly fresh allanite and undergoing dissolution. Note sparry nature of a portion of the grain (arrow). Grain from the Coleman River Formation sample C9-7.

this value was determined at pH = 1.4; Rose 1991). Etch pit nucleation is favored on surface sites of excess strain energy, in highly undersaturated solutions (Blum and Lasaga 1987). Surface sites of excess energy include twin boundaries and intersections of dislocations with crystal surfaces (Berner 1978, 1981; Brantley et al. 1986; Blum and Lasaga 1987). The presence of line defects intersecting the mineral surface facilitates the migration of molecular water into the crystal (Schott and Petit 1987).

Several crystal-chemical factors may contribute to the resistance of epidote to weathering. The Fe in epidote is Fe_2O_3, which will almost certainly render epidote less vulnerable to weathering in oxidizing environments than other common silicates with ions vulnerable to oxidation (e.g., FeO in olivines and pyroxenes). Additionally, Velbel (1999) has shown that bond energetics of non-tetrahedral cations explain much of the relative resistance to weathering of different orthosilicates. This may apply to more complex silicates as well. In this connection, Smyth and Bish (1988, their Table 5.1.3) reported octahedral site energies for Al sites in epidote that are as low as or even lower than the very lowest for orthosilicates (as reviewed by Velbel 1999). Some octahedral Al-bearing sites in epidote are more energetically stable (and resistant to removal of Al) than the corresponding sites in the most weathering-resistant Al-bearing orthosilicates. Low energies for Al-containing sites may contribute to the resistance of epidote to weathering.

In contrast to epidote, allanite weathering is rapid, with complete dissolution occurring below the weathering front. The only other mineral in this study displaying any evidence of weathering during allanite dissolution is biotite, similar to studies elsewhere (e.g., Delvigne 1998). Metamictization is likely the dominant reason for the preferential weatherablility of allanite relative to epidote, but two other factors may contribute to enhanced weathering of allanite relative to epidote. (1) The Fe in allanite includes appreciable FeO, which is subject to oxidation in common weathering environments. (2) The energies for Fe-bearing sites in allanite are higher than in epidote (Smyth and Bish 1988, their Table 5.1.3). The Fe in allanite is subject to oxidation (in contrast to the Fe in epidote), and the Fe-bearing site in allanite is more easily disrupted than the corresponding site in epidote. By virtue of these crystal-chemical differences, even young or otherwise non-metamict allanites might be expected to weather more readily than epidote, as observed in this study.

Allanite weathering may not have been previously recognized at Coweeta and elsewhere for several reasons. First, allanite grains are small and occur as accessory phases in unweathered rock. Even if recognized, their small abundances may preclude them from being included with other weatherable minerals that occur in much larger quantities (e.g., plagioclase and biotite). Second, allanite may not be distinguishable from epidote in thin section, as is the case in unweathered bedrock at Coweeta. Epidote is generally regarded as being relatively unweatherable, and has been compared to quartz and zircon (e.g., Allen and Hajek 1995; Lång 2000). The interpretation of epidote being relatively unweatherable is especially true if epidote-group minerals are identified in the bedrock, with epidote being noted in the solum. Such observations could easily lead to the conclusion that the epidote-group minerals noted in the bedrock are actually epidote, and are relatively unweatherable. Finally, allanite weathers so rapidly below the weathering front that it is difficult to locate grains that display evidence of weathering.

Because allanite and epidote may be indistinguishable in thin section, allanite weathering may be mistaken for epidote weathering. Sverdrup (1990), Warfvinge and Sverdrup (1992), Sverdrup and Warfvinge (1993, 1995), and Oliva et al. (2004) may be correct in invoking weathering of epidote-group minerals (rather than epidote specifically), if the actual mineral weathering is allanite. However, microscopic observations and analytical data would need to be provided to support such a conclusion.

At Coweeta, allanite dissolution has been invoked as an important source of Ca to stream waters. Elsewhere, however additional mineralogic sources of Ca to stream waters include calcite (e.g., Velbel 1992; Blum et al. 1998; White et al. 1999; Taylor et al. 2000a, 2000b), apatite (e.g., Aubert et al. 2001, 2002; Blum et al. 2002; Oliva et al. 2004), and trace calc-silicate phases (i.e., epidote, prehnite, and bytownite; Oliva et al. 2004). Aubert et al. (2001, 2002) utilized Sr and Nd isotopic data, in combination with REE data, of springwaters from the Strengbach catchment in the Vosges Mountains of France, and determined that the springwater chemistry reflected a 15% contribution from apatite weathering. Similarly, from Sr isotope and Ca data of stream water draining a watershed located at Hubbard Brook Experimental Forest located in New Hamsphire, Blum et al. (2002) estimated that approximately 35% of the Ca was derived from the weathering of apatite. Accessory calcite dissolution during weathering of silicate rocks may also contribute significant quantities of Ca to stream waters (e.g. Velbel 1992), but is primarily a concern for recently glaciated or tectonically active landscapes (Blum et al. 1998; White et al. 1999). Blum et al. (1998) found that trace amounts (~1%) of calcite found within granitoid rocks control stream water chemistry of glaciated northern Pakistan. Disseminated calcite in exfoliated granitoid rocks of recently glaciated (<10 Ka), high-elevation watersheds located in the western USA, contributes between 31 and 85 mol% Ca in discharge fluxes (White et al. 1999). In contrast, White et al. (1999) also found that watersheds located

in geomorphically older landscapes (>200 Ka) such as Georgia, and Rio Icacos (Puerto Rico), did not exhibit Ca excesses beyond that explained by plagioclase weathering. Experimental studies of plagioclase and mica weathering have also concluded that in silicate-weathering environments, the dissolution of disseminated calcite is limited by mechanical processes such as glaciation and tectonism that result in exposure of unweathered calcite to weathering solutions (Taylor et al. 2000a, 2000b). Recently, Oliva et al. (2004) studied the high-elevation Estibère watershed in the French Pyrenees. They found that the trace calcic minerals apatite, epidote, prehnite, and bytownite, which represent ~1 vol% of the rock, are responsible for more than 80% of the Ca export from the watershed. The remaining Ca loss was attributed to oligoclase weathering. Oliva et al. (2004) did note allanite, as well as hornblende and actinolite, being present in the watershed bedrock, but did not invoke their weathering to be significant in the Ca budget.

ACKNOWLEDGMENTS

The authors wish to thank the Coweeta Hydrological Laboratory staff, including W. Swank and J. Knoepp, who provided splits of core samples to the second author, and provided assistance and suggestions during field activities. Comments made by reviewers S. Wood and J. Blum greatly enhanced the quality of this manuscript. Thanks, too, to J. Ayers for his editorial assistance. Funding for this project was partially provided by a Grant-in-Aid of Research, from Sigma Xi, The Scientific Research Society, Michigan Space Grant Consortium Graduate Fellowship, and Clay Minerals Society Student Grant.

REFERENCES CITED

Allen, B.L. and Hajek, B.F. (1995) Mineral occurrence in soil environments. In J.B. Dixon and S.B. Weed, Eds., Minerals in Soil Environments (Second edition), p. 199–278. Soil Science Society of America Book Series No. 1, Madison, Wisconsin.

Aubert, D., Stille, P., and Probst, A. (2001) REE fractionation during granite weathering and removal by waters and suspended loads: Sr and Nd isotopic evidence. Geochimica et Cosmochimca Acta, 65, 387–406.

Aubert, D., Stille, P., Probst, A., Gauthier-Lafaye, F., Pourcelot, L., and Delnero, M. (2002) Characterization and migration of atmospheric REE in soils and surface waters. Geochimica et Cosmochimica Acta, 66, 3339–3350.

Banfield, J.F. and Eggleton, R.A. (1989) Apatite replacement and rare earth mobilization, fractionation, and fixation during weathering. Clays and Clay Minerals, 37, 113–127.

Barman, A.K., Varadachari, C., and Ghosh, K. (1992) Weathering of silicate minerals by organic acids. I. Nature of cation solubilisation. Geoderma, 53, 45–63.

Berner, R.A. (1978) Rate control of mineral dissolution under earth surface conditions. American Journal of Science, 278, 1235–1252.

——— (1981) Kinetics of weathering and diagenesis. In A.C. Lasaga and R.J. Kirkpatrick, Eds., Kinetics of Geochemical Processes, 8, p. 111–134. Reviews in Mineralogy, Mineralogical Society of America, Washington, D.C.

Berner, R.A., and Holdren, G.R., Jr. (1977) Mechanism of feldspar weathering: some observational evidence. Geology, 5, 369–372.

——— (1979) Mechanism of feldspar weathering—II. Observations of feldspars from soils. Geochimica et Cosmochimica Acta, 43, 1173–1186.

Berry, J.L. (1976) Study of chemical weathering in the Coweeta Hydrologic Laboratory, Macon County, North Carolina, 62 p. Unpublished report.

Blum, A.E. and Lasaga, A.C. (1987) Monte Carlo simulations of surface reaction rate laws. In W. Stumm, Ed., Aquatic Surface Chemistry, p. 255–292. John Wiley & Sons, New York.

Blum, J.D., Gazis, C.A., Jacobson, A.D., and Chamberlain, C.P. (1998) Carbonate versus silicate weathering in the Raikhot watershed within the High Himalayan Crystalline Series. Geology, 26, 411–414.

Blum, J.D., Klaue, A., Nezat, C.A., Driscoll, C.T., Johnson, C.E., Siccama, T.G., Eager, C., Fahey, T., and Likens, G.E. (2002) Mycorrhizal weathering of apatite as an important calcium source in base-poor forest ecosystems. Nature, 417, 729–731.

Bowser, C.J. and Jones, B.F. (1993) Mass balances of natural water: Silicate dissolution, clays, and the calcium problem. Biogeomon Symposium on Ecosystem Behavior: Evaluation of Integrated Monitoring in Small Catchments, Prague, Czech Republic, 30–31.

——— (2002) Mineralogic controls on the composition of natural waters dominated by silicate hydrolysis. American Journal of Science, 32, 582–662.

Brantley, S.L., Crane, S.R., Crerar, D.A., Hellmann, R., and Stallard, R. (1986) Dissolution at dislocation etch pits in quartz. Geochimica et Cosmochimica Acta, 50, 2349–2361.

Braun, J.-J. and Pagel, M. (1994) Geochemical and mineralogic behavior of REE, Th, and U in the Akongo lateritic profile (SW Cameroon). Catena, 21, 173–177.

Braun, J-J., Pagel, M., Muller, J.P., Bilong, P., Michard, A., and Guillet, B., (1990) Cerium anomalies in lateritic profiles. Geochimica et Cosmochimica Acta, 51, 597–605.

Braun, J-J., Pagel, M., Herbillon, A., and Rosin, C. (1993) Mobilization and redistribution of REE and thorium in a syenitic lateritic profile: a mass balance study. Geochimica et Cosmochimica Acta, 57, 4419–4434.

Braun, J.-J., Viers, J., Dupré, B., Ndam, J., and Muller, J.-P. (1998) Solid/liquid REE fractionation in the lateritic system of Goyoum, East Cameroon: the implications for the present dynamics of the soil covers of the humid tropical regions. Geochimica et Cosmochimica Acta, 62, 273–299.

Bromley, A.V. (1964) Allanite in the Tan-Y-Grisiau microgranite, Merionethshire, North Wales. American Mineralogist, 49, 1747–1754.

Burt, D.M. (1989) Compositional and phase relations among rare earth element minerals. In B.R. Lipin and G.A. McKay, Eds., Geochemistry and Mineralogy of Rare Earth Elements, 21, p. 259–308. Reviews in Mineralogy, Mineralogical Society of America, Washington, D.C.

Carver, R.E. (1986) Rates of intrastratal solution of heavy minerals in southeast Atlantic Coastal Plain and their potential of dating sedimentary events. American Association of Petroleum Geologists Bulletin, 70, 572.

Ciampone, M.A. (1995) Non-systematic weathering profile on metamorphic rock in the southern Blue Ridge Mountains, North Carolina: Petrography, bulk chemistry, and mineral chemistry of biotite [unpublished M.S. thesis], 86 p. University of Cincinnati, Cincinnati, Ohio.

Cocker, M.D. (1998) Defining the heavy mineral potential in the upper coastal plain of Georgia with the use of NURE stream sediment geochemical data and a geographical information system. 33rd Forum on the Geology of Industrial Minerals, Proceedings, Canadian Institute on Mining and Metallurgy Special Volume 50, Montreal, 131–144.

Cotton, J., Le Dez, A., Bau, M., Carott, M., Maury, R.C., Dulski, P., Fourcade, S., Bohn, M., Brousse, R. (1995) Origin of anomalous rare-earth element and yttrium enrichments in subaerially exposed basalts: evidence from French Polynesia. Chemical Geology, 119, 115–38.

Deer, W.A., Howie, R.A., and Zussman, J. (1986) Rock-Forming Minerals, Volume 1B, Disilicates and Ring Silicates, 629 p. Wiley, New York.

Delvigne, J.E. (1998) Atlas of Micromorphology of Mineral Alteration and Weathering, 494 p. The Canadian Mineralogist Special Publication 3, Mineralogical Association of Canada, Ottawa, Ontario.

Dill, H.G. (1995) Heavy mineral response to the progradation of an alluvial fan: implications concerning unroofing of source area, chemical weathering and palaeo-relief (Upper Cretaceous Parkstein fan complex, SE Germany). Sedimentary Geology, 95, 39–56.

Dollase, W.A. (1971) Refinement of the crystal structure of epidote, allanite and Hancockite. American Mineralogist, 56, 447–464.

Drever, J.I. (1997a) Catchment mass balance. In O.M.Saether and P. de Caritat, Eds., Geochemical Processes, Weathering and Ground water Recharge in Catchments, p. 241–261. A.A. Balkema, Rotterdam, Netherlands.

——— (1997b) The Geochemistry of Natural Waters: Surface and Ground water Environments (3rd edition), 436 p. Prentice Hall, New Jersey.

Ercit, T.S. (2002) The mess that is "allanite". The Canadian Mineralogist, 40, 1411–1419.

Ewing, R.C. (1976) Metamict mineral alteration: an implication for radioactive waste disposal. Science, 192, 1336–1337.

Ewing, R.C. and Haakar, R.F. (1981) Amorphous structure of metamict minerals observed by TEM. Nature, 293, 449–450.

Ezzaïm, A., Turpault, M.-P., and Ranger, J. (1999) Quantification of weathering processes in an acid brown soil developed from tuff (Beaujolais, France) Part I., Formation of weathered rind. Geoderma, 87, 137–154.

Friis, H. (1974) Weathered heavy-mineral associations from the young-Tertiary deposits of Jutland, Denmark. Sedimentary Geology, 12, 199–213.

Frondel, J.W. (1964) Variation of some rare earths in allanite. American Mineralogist, 49, 1159–1177.

Frye, J.C., William, H.B., and Glass, H.D. (1960) Gumbotil, Accretion-Gley, and the Weathering Profile, 39 p. Illinois State Geological Survey Circular 295.

Fryer, B.J., Jackson, S.E., and Longerich, H.P. (1995) The design, operation and role of the laser-ablation microprobe coupled with inductively coupled plasma-mass spectrometer (LAM-ICP-MS) in the earth sciences. The Canadian Mineralogist, 33, 303–312.

Gavshin, V.M., Shcherbov, B.L., Bobrov, V.A., Solotchina, E.P., Sukhorukov, F.V., and Mel'gunov, M.S. (1997) Behavior of trace elements in the process of formation of a weathering profile on granites. Russian Geology and Geophysics, 38, 1264–1276.

Goldich, S.S. (1938) A study in rock-weathering. Journal of Geology, 46, 17–58.

Grauch, R.I. (1989) Rare Earth elements in metamorphic rocks. In B.R. Lipin and G.A. McKay, Eds., Geochemistry and Mineralogy of Rare Earth Elements, 21, p. 147–168. Reviews in Mineralogy, Mineralogical Society of America, Washington, D.C.

Gromet, L.P., and Silver, L.T. (1983) Rare earth element distributions among minerals in a granodiorite and their petrogenetic implications. Geochimica et Cosmochimica Acta, 47, 925–939.

Gupta, R.K. and Talwar, C.L. (1997) Mineralogy of soils developed on Karewas in Baramula and Kupwara areas of Kashmir. Clay Research, 16, 31–34.

Harlavan, Y. and Erel, Y. (2002) The release of Pb and REE from granitoids by the dissolution of accessory phases. Geochimica et Cosmochimica Acta, 66, 837–848.

Hata, S. (1939) The alteration of allanite. Scientific Papers of the Institute of Physical and Chemical Research, 36, 301–311.

Hatcher, R.D. (1980) Geologic map of Coweeta Hydrologic Laboratory, Prentiss Quadrangle, North Carolina, scale 1:14,400. State of North Carolina, Department of Natural Resources and Community Development, in Cooperation with the Tennessee Valley Authority.

——— (1988) Bedrock geology and regional geologic setting of Coweeta Hydrologic Laboratory in the Eastern Blue Ridge. In W.T. Swank and D.A. Crossley, Jr., Eds., Forest Hydrology and Ecology at Coweeta, p. 81–92. Springer-Verlag, New York.

Hermann, J. (2002) Allanite: thorium and light rare earth element carrier in subducted crust. Chemical Geology, 192, 289–306.

Hochella, M.F. and Banfield, J.F. (1995) Chemical weathering of silicates in nature: a microscopic perspective with theoretical considerations. In A.F. White and S.L. Brantley, Eds., Chemical Weathering Rates of Silicate Minerals, 31, p. 353–406. Reviews in Mineralogy, Mineralogical Society of America, Washington, D.C.

Jackson, S.E., Longerich, H.P., Dunning, G.R., and Fryer, B.J. (1992) The application of laser ablation microprobe-inductively coupled plasma-mass spectrometry (LAM-ICP-MS) to in situ trace element determination in minerals. The Canadian Mineralogist, 30, 1049–1064.

Jacobson, A.D., Blum, J.D., Chamberlain, C.P., Craw, D., and Koons, P.O. (2003) Climatic and tectonic controls on chemical weathering in the New Zealand Southern Alps. Geochimica et Cosmochimica Acta, 67, 29–46.

Janeczek, J. and Eby, R.K. (1993) Annealing of radiation damage in allanite and gadolinite. Physics and Chemistry of Minerals, 19, 343–356.

Jeffries, T.E., Perkins, W.T., and Pearce, N.J.G. (1995) Measurements of trace elements in basalts and their phenocrysts by laser probe microanalysis inductively coupled plasma mass spectrometry (LPMA-ICP-MS). Chemical Geology, 121, 131–144.

Jenner, G.A., Foley, S.F., Jackson, S.E., Green, T.H., Fryer, B.J., and Longerich, H.P. (1993) Determination of partition coefficients for trace elements in high pressure-temperature experimental run products by laser ablation microprobe-inductively coupled plasma-mass spectrometry (LAM-ICP-MS). Geochimica et Cosmochimica Acta, 57, 5099–5103.

Kalinowski, B.E., Faith-Ell, C., and Schweda, P. (1998) Dissolution kinetics and alteration of epidote in acidic solutions at 25°C. Chemical Geology, 151, 181–197.

Keller, W.D. (1976) Scan electron micrographs of kaolins collected from diverse environments of origin: I. Clays and Clay Minerals, 24, 107–113.

——— (1978) Kaolinization of feldspar as displayed in scanning electron micrographs. Geology, 6, 184–188.

Khan, A.M. and Kim, S.J. (1998) Control of physico-chemical conditions on the mineralogical characteristics of weathering profile of anorthositic rocks of Suryun area, Korea. Acta Mineralogica Pakistanica, 9, 1–6.

Klein, C. and Hurlbut, C.S. (1999) Manual of Mineralogy, 681 p. John Wiley & Sons, Inc., New York.

Koppi, A.J., Edis, R., Field, D.J., Geering, H.R., Klessa, D.A., and Cockayne, D.J.H. (1996) Rare earth element trends and cerium-uranium-manganese associations in weathered rock from Koongarra, Northern Territory, Australia. Geochimica et Cosmochimica Acta, 60, 1695–1707.

Lång, L.-O. (2000) Heavy mineral weathering under acidic soil conditions. Applied Geochemistry, 15, 415–423.

Lasaga, A.C. (1984) Chemical kinetics of water-rock interactions. Journal of Geophysical Research, 89, 4009–4025.

Logan, W.S. and Dyer, L.J. (1996) Influence of mineral weathering reactions, road salt and cation exchange on ground water chemistry, Catoctin Mountain, Central Maryland. Geological Society of America Abstracts with Programs, 28, 31–32.

Longerich, H.P., Jackson, S.E., and Gunther, D. (1996) Laser ablation inductively coupled plasma mass spectrometric transient signal data acquisition and analyte concentration calculation. Journal of Analytical Atomic Spectrometry, 11, 899–904.

Meintzer, R.E. (1981) Thorium and rare earth element migration incipient to the weathering of an allanite pegmatite, Amherst County, Virginia [unpublished M.S. thesis], 107 p. University of Virginia, Charlottesville, Virginia.

Miller, C.F., Hatcher, R.D., Jr., Ayers, J.C., Coath, C.D., and Harrison, T.M. (2000) Age and zircon inheritance of eastern Blue Ridge plutons, southwestern North Carolina and northeastern Georgia, with implications for magma history and evolution of the southern Appalachian orogen. American Journal of Science, 300, 142–172.

Mills, H.H., Brackenridge, G.R., Jacobson, R.B., Newell, W.L., Pavich, M., and Pomery, J.S. (1987) Appalachian mountains and plateaus, In W.L. Graf, Ed., Geomorphic Systems of North America, 2, p. 5–50. Geological Society of America Centennial Special Volume, Boulder, Colorado.

Mitchell, R.S. (1966) Virginia metamict minerals: allanite. Southeastern Geology, 7, 183–195.

Nagy, K.L. (1995) Dissolution and precipitation kinetics of sheet silicates. In A.F. White and S.L. Brantley, Eds., Chemical Weathering Rates of Silicate Minerals, 31, p. 173–234. Reviews in Mineralogy, Mineralogical Society of America, Washington, D.C.

Neal, C.R., Davidson, J.P., and McKeegan, K.D. (1995) Geochemical analysis of small samples: micro-analytical techniques for the nineties and beyond. Reviews in Geophysics, Supplement, 25–32.

Nesbitt, H.W. and Markovics, G. (1997) Weathering of granodiorite crust, long-term storage of elements in weathering profiles, and petrogenesis of siliclastic sediments. Geochimica et Cosmochimca Acta, 61, 1653–1670.

Nickel, E. (1973) Experimental dissolution of light and heavy minerals in comparison with weathering and intrastratal solution. Contributions to Sedimentology, 1, 1–68.

Norman, M.D., Pearson, N.J., Sharma, A., and Griffin, W.L. (1996) Quantitative analysis of trace elements in geological materials by laser ablation ICPMS: Instrumental operating conditions and calibration values of NIST glasses. Geostandards Newsletter, 20, 247–261.

Oliva, P., Dupré, B., Martin, F., and Viers, J. (2004) The role of trace minerals in chemical weathering in a high-elevation granitic watershed (Estibère, France): Chemical and mineralogical evidence. Geochimica et Cosmochimica Acta, 68, 2223–2244.

Palmquist, J.C. (1990) Metamict allanite in Archean gneiss, Bighorn Mountains, Wyoming. Geological Society Abstracts with Programs, 22, 41.

Patino, L.C., Velbel, M.A., Price, J.R., and Wade, J.A. (2003) Trace element mobility during spheroidal weathering of basalts and andesites in Hawaii and Quatemala. Chemical Geology, 202, 343–364.

Peng, M. and Ruan, D. (1986) A spectroscopic study on the allanite from a granite body in northeastern Guangdong. Journal of Central-South Institute of Mining and Metallurgy, 1, 1–9.

Perkins, W.T., Pearce, N.J.G., and Jeffries, T.E. (1993) Laser ablation inductively coupled plasma mass spectrometry: a new technique for the determination of trace element and ultra-trace elements in silicates. Geochimica et Cosmochimica Acta, 57, 475–482.

Poitrasson, F., Paquette, J.-L., Montel, J.-M., Pin, C., and Duthou, J.-L. (1998) Importance of late-magmatic and hydrothermal fluids on the Sm-Nd isotope mineral systematics of hypersolvus granites. Chemical Geology, 146, 187–203.

Poppe, L.J., Commeau, J.A., and Luepke, G. (1995) Silt fraction heavy-mineral distributions in a lateritic environment: the rivers and insular shelf of north-central Puerto Rico. Sedimentary Geology, 95, 251–268.

Ramspott, L.D. (1965) Earliest effects of weathering in Elberton Granite. Bulletin of the Georgia Academy of Science, 23, 34–35.

Rose, N.M. (1991) Dissolution rates of prehnite, epidote and albite. Geochimica et Cosmochimica Acta, 55, 3273–3286.

Schalscha, E.B., Appelt, H., and Schaltz, A. (1967) Chelation as a weathering mechanism—I. Effect of complexing agents on the solubilization of iron from minerals and granodiorite. Geochimica et Cosmochimica Acta, 31, 587–596.

Schott, J. and Petit, J.-C. (1987) New evidence for the mechanisms of dissolution of silicate minerals. In W. Stumm, Ed., Aquatic Surface Chemistry, p. 255–292. Wiley, New York.

Schroeder, P.A., Melear, N.D., West, L.T., and Hamilton, D.A. (2000) Meta-gabbro weathering in the Georgia Piedmont, USA: implications for global silicate weathering rates. Chemical Geology, 163, 235–245.

Schwertmann, U. and Taylor, R.M. (1995) Iron oxides. In J.B. Dixon and S.B. Weed, Eds., Minerals in Soil Environments (Second edition), p. 379–438. Soil Science Society of America Book Series No. 1, Madison, Wisconsin.

Smyth, J.R. and Bish, D.L. (1988) Crystal Structures and Cation Sites of the Rock-Forming Minerals. 332 pp. Allen & Unwin, Boston, Massachusettes.

Strens, R.G.J. (1966) Properties of the Al-Fe-Mn epidotes. Mineralogical Magazine, 25, 928–944.

Sun, S.-S. and McDonough, W.F. (1989) Chemical and isotopic systematics of oceanic basalts: implications for mantle composition and processes. In A.D. Saunders and M.J. Norry, Eds., Magmatism in the Ocean Basins, 42, p. 313–345. Geological Society Special Publication.

Suwa, K., Matsuzawa, I., Iida, C., and Yamasaki, K. (1958) Mineralogical and geochemical studies on the weathering of a quartz porphyry. The Journal of Earth Sciences, Negoya University, 6, 75–100.

Sverdrup, H.U. (1990) The Kinetics of Base Cation Release due to Chemical Weathering, 246 p. Lund University Press, Lund, Sweden.

Sverdrup, H. and Warfvinge, P. (1993) Calculating field weathering rates using a mechanistic geochemical model PROFILE. Applied Geochemistry, 8, 273–283.

Sverdrup, H. and Warfvinge, P. (1995) Estimating weathering rates using laboratory kinetics: In A.F. White and S.L. Brantley, Eds., Chemical Weathering Rates of Silicate Minerals, 31, 485–542. Reviews in Mineralogy, Mineralogical Society of America, Washington, D.C.

Taylor, A.S., Blum, J.D., and Lasaga, A.C. (2000a) The dependence of labradorite dissolution and Sr isotope release rates on solution saturation state. Geochimica et Cosmochimica Acta, 64, 2389–2400.

Taylor, A.S., Blum, J.D., Lasaga, A.C., and MacInnis, I.N. (2000b) Kinetics of dissolution and Sr release during biotite and phlogopite weathering. Geochimica et Cosmochimica Acta, 64, 1191–1208.

Taylor, G. and Eggleton, R.A. (2001) Regolith Geology and Geomorphology, 375 p. John Wiley & Sons, Ltd., New York.

Uddin, A. and Lundberg, N. (1998) Unroofing history of the eastern Himalaya and the Indo-Burman ranges: heavy-mineral study of Cenozoic sediments from the Bengal Basin, Bangladesh. Journal of Sedimentary Research, 68, 465–472.

van der Weijden, C.H. and van der Weijden, R.D. (1995) Mobility of major, minor and some redox-sensitive trace elements and rare-earth elements during weathering of four granitoids in central Portugal. Chemical Geology, 125, 149–167.

Varadachari, C., Barman, A.K., and Ghosh, K. (1992) Weathering of silicate minerals by organic acids II. Nature of residual products. Geoderma, 61, 251–268.

Velbel, M.A. (1983) A dissolution-reprecipitation mechanism for the pseudomorphous replacement of plagioclase feldspar by clay minerals during weathering. Science Géologie Mémoires, 71, 139–147.

——— (1984) Natural weathering mechanisms of almandine garnet. Geology, 12, 631–634.

——— (1985) Geochemical mass balances and weathering rates in forested watersheds of the southern Blue Ridge. American Journal of Science, 285, 904–930.

——— (1986) Influence of surface area, surface characteristics, and solution composition on feldspar weathering rates. In J.A. Davis and K.F Hayes, Eds., Geochemical Processes at Mineral Surfaces, 323, p. 615–634. American Chemical Society Symposium Series, Washington, D.C.

——— (1988) Weathering and soil-forming processes. In W.T. Swank and D.A. Crossley, Jr., Eds., Forest Hydrology and Ecology at Coweeta, p.93–102. Springer-Verlag, New York.

——— (1990) Mechanisms of saprolitization, isovolumetric weathering, and pseudomorphous replacement during rock weathering—a review. Chemical Geology, 84, 17–18.

——— (1992) Geochemical mass balances and weathering rates in forested watersheds of the southern Blue Ridge, III. Cation budgets and the weathering rate of amphibole. American Journal of Science, 292, 58–78.

——— (1993) Formation of protective surface layers during silicate-mineral weathering under well-leached, oxidizing conditions. American Mineralogist, 78, 405–414.

——— (1999) Bond strength and the relative weathering rates of simple orthosilicates. American Journal of Science, 299, 679–696.

Velbel, M.A., Basso, C.L., and Zieg, M.J. (1996) The natural weathering of staurolite: Crystal-surface textures, relative stability, and the rate-determining step. American Journal of Science, 296, 453–472.

Warfvinge, P. and Sverdrup, H. (1992) Calculating critical loads of acid deposition with PROFILE—A steady-state soil chemistry model. Water, Air, Soil Pollution, 63, 119–143.

Watson, T.L. (1917) Weathering of allanite. Bulletin of the Geological Society of America, 28, 463–500.

White, A.F., Bullen, T.D., Vivit, D.V., Schulz, M.S., and Clow, D.W., (1999) The role of disseminated calcite in the chemical weathering of granitoid rocks. Geochimica et Cosmochimica Acta, 63, 1939–1953.

Willman, H.B., Glass, H.D., and Frye, J.C. (1963) Mineralogy of Glacial Tills and Their Weathering Profiles in Illinois, Part I. Glacial Tills, 55 p. Illinois State Geological Survey Circular 347.

Wilson, A.F. (1966) Metamict allanite from pegmatites cutting basic charnockitic granulites in the Fraser Range, Western Australia. Journal of the Royal Society of Western Australia, 49, 85–87.

Wilson, M.J. (1975) Chemical weathering of some primary rock-forming minerals. Soil Science, 119, 349–355.

Wood, S.A. and Ricketts, A. (2000) Allanite-(Ce) from the Eocene Casto granite, Idaho: response to hydrothermal alteration. The Canadian Mineralogist, 38, 81–100.

Yeakley, J.A., Swank, W.T., Swift, L.W., Hornberger, G.M., and Shugart, H.H. (1998) Soil moisture gradients and controls on a southern Appalachian hillslope from drought through recharge. Hydrology and Earth System Sciences, 2, 41–49.

MANUSCRIPT RECEIVED AUGUST 16, 2003
MANUSCRIPT ACCEPTED AUGUST 1, 2004
MANUSCRIPT HANDLED BY JOHN AYERS